

Chiral model of the nucleon: Projecting the hedgehog as a coherent state

Michael C. Birse*

*Institute for Nuclear Theory, Department of Physics, FM-15,
University of Washington, Seattle, Washington 98195*

(Received 10 May 1985)

The construction of baryon states with good spin and isospin is studied in a chiral model. This is a linear σ model, describing quarks interacting with pions and σ mesons. It has previously been investigated in the mean-field approximation (MFA), using the hedgehog ansatz. The ansatz corresponds to a mixture of spin-isospin eigenstates. A coherent state is used to provide a quantum description for the mesonic part of the wave function. The hedgehog baryon is projected onto states with good spin and isospin. The Peierls-Yoccoz projection is used, in analogy with the treatment of deformed nuclei. As well as N and Δ , a $J = T = \frac{5}{2}$ baryon state is obtained. The wave functions are varied after projection. For the N and Δ , the resulting field distributions are fairly similar to those from the MFA. Various nucleon properties are calculated. These include proton and neutron charge radii, for which reasonable agreement with experiment is obtained. Results for other properties are similar to those obtained with an approximate projection method, and indicate the need to extend the present approach to include vector mesons and the effects of vacuum polarization. Comparisons are made with wave functions used in the cloudy bag and Skyrme models.

I. INTRODUCTION

Although quantum chromodynamics¹ (QCD) is now believed to be the underlying theory of the strong interaction, its long-distance, nonperturbative regime has so far defied solution. Lattice gauge calculations² have provided some information on this regime. However, the restrictions imposed by available computers make this approach best suited to calculating bulk properties of the QCD vacuum and phase transitions. The best hope of relating hadronic properties and interactions to QCD continues to be the use of models or effective theories containing degrees of freedom appropriate to the long-distance regime. Such degrees of freedom include "constituent quarks," meson, and "glueball" fields. Eventually, one would like to determine the parameters of these models from first principles, for example, from lattice gauge calculations. For the moment, these parameters must be fixed phenomenologically.

Recently there has been much interest in so-called soliton models.³ Many of these models are similar in spirit to the Lee-Wick model of abnormal nuclear matter.⁴ The solitons are stabilized by coupling to fermion fields. They consist of quarks interacting with various phenomenological boson fields which are introduced to describe the long- and intermediate-range properties of QCD (Refs. 5–12).

An alternative type of soliton model, first proposed by Skyrme,¹³ is based on the nonlinear σ model and does not include explicit quark degrees of freedom.^{14–16} Instead the model has a conserved topological winding number which is interpreted as the baryon number. Stability is achieved with higher-order derivative interactions^{13,14} or by coupling to vector mesons.¹⁶

Most existing calculations in these models use the semiclassical or mean-field approximation (MFA). This treats the boson fields as classical and neglects the effects of quantum fluctuations. In models with quarks, only

valence quarks are included, but these are treated quantum mechanically. This approximation is, in many respects, similar to the Hartree-Fock approximation used in nuclear and atomic physics.

The static, localized solutions to the resulting nonlinear field equations are referred to as *solitons*.^{17,18} Since they are localized, these solutions break the translational symmetry of the corresponding field theories. Models with chiral symmetry are generally studied using the "hedgehog" ansatz.¹⁹ This violates the rotational and isospin symmetries of the model as well as the translational.

The symmetries of the model which are broken by the semiclassical solution correspond to degeneracies of the soliton. Each degeneracy gives rise to a spurious zero-energy state in the excitation spectrum built on the soliton. These "zero modes" give rise to infrared divergences in the loop diagrams used to evaluate fluctuations about the mean field. Analogous problems with spurious states occur in Hartree-Fock calculations of nuclei.²⁰

Another way of seeing the problem is to consider the generators of the symmetries broken by the soliton. For example, in a hedgehog state the expectation value of the total angular momentum vanishes:

$$\langle H | \mathbf{J} | H \rangle = 0. \quad (1.1)$$

The quarks, if present, are in states which contain an equal mixture of spin up and down (see Sec. II for details) and there is no contribution to (1.1) from the static mean pion field. Since the hedgehog is not an eigenstate of total angular momentum, both quarks and pions can contribute to the expectation value of J^2 via quantum fluctuations. Hence we have

$$\langle H | J^2 | H \rangle > 0. \quad (1.2)$$

Similar results hold for the linear momentum because a localized soliton breaks translational invariance.²¹

Ideally, one would like to separate the collective degrees of freedom (conjugate variables to the generators of the broken symmetries) from those describing the intrinsic motion. However, even in many-body systems, such a separation is by no means trivial, and is often not very useful since the collective and intrinsic motions remain strongly coupled.²² Various similar approaches have been used to describe soliton motions in quantum field theories but, even for simple one-dimensional models, these methods become very complicated.²³

The most practical way to handle collective motions (both in many-body and field theories) seems to be the use of generator coordinates.²⁴ As applied to the construction of states with the correct symmetries this is usually known as the Peierls-Yoccoz projection.²⁵ It involves taking linear combinations of all the degenerate, broken-symmetry states obtained from the MFA:

$$|\Psi\rangle = \int d\alpha f(\alpha) |\Phi(\alpha)\rangle, \quad (1.3)$$

where the $|\Phi(\alpha)\rangle$ are the degenerate states, labeled by a set of continuous "generator coordinates" α . With an appropriate choice of the weight function $f(\alpha)$ the state $|\Psi\rangle$ will be an eigenstate of the generators of the symmetries which are broken in the soliton states $|\Phi(\alpha)\rangle$.

In order to use the generator-coordinate method we need a complete wave function describing the soliton state. But the MFA provides only classical field configurations for the boson fields; these are interpreted as the expectation values in the state of interest. The simplest choice of wave function which reproduces many of the features of the MFA is the *coherent state*.^{26–29} This is essentially a Gaussian wave packet in the function space of the quantum field theory, and is peaked at the field configuration which corresponds to the classical mean field. The detailed form of such a state is described in Sec. II.

This method (construction of a coherent state and projection) has previously been used^{30,21} to obtain eigenstates of linear momentum in the soliton bag model.^{6,18} Here I apply it to the construction of states with good spin and isospin in a chiral soliton model^{8,9} (with quarks). Recently, two groups have made similar calculations³¹ in the cloudy bag model.³²

It should be noted that this method can only be applied to models in which the boson fields are canonically quantizable. Hence it cannot be used in the Skyrme model.^{13–16} The nonlinear constraint on the pion fields in this model means that it is defined over a curved function space.³³ Thus it cannot be quantized in the usual canonical way, except in the linearized approximation used in the cloudy bag model.³² The evaluation of loop diagrams³⁴ is much more complicated than in the linear σ model and, of course, the model is nonrenormalizable. The projection technique described here introduces into the wave function large amplitude fluctuations associated with the rotational degeneracy of the soliton. In a nonlinear model it would be essential to take account of the curvature of the function space. The simple Gaussian coherent state, which could be used to describe small amplitude fluctuations in the linear approximation, is thus not an appropriate starting point for projection in this

model. In the absence of a suitable wave function, Adkins *et al.*¹⁴ assume that the hedgehog can be regarded as the intrinsic state of a rigid rotor and they treat quantum mechanically only the rotational motion. This approach will be discussed again in Sec. VII.

The model^{8,9} which I use here is based on the linear σ model of Gell-Mann and Lévy.³⁵ It describes an isospin doublet of quarks interacting with pions and scalar, isoscalar mesons. The quark-meson coupling maintains the (approximate) $SU(2) \times SU(2)$ chiral symmetry of the underlying theory, QCD. The self-interactions of the mesons are chosen so that the chiral symmetry is realized in the hidden mode (also known as the spontaneously broken or Nambu-Goldstone mode). The σ field has a nonzero vacuum expectation value, which gives the quarks a large dynamical mass, while the pions are massless Goldstone bosons (or are light if the symmetry is only approximate).

The motivation for this model is described in Ref. 8. It is based on the idea of a separation of roles between the forces which bind quarks into hadrons and those which lead to confinement.^{36–38} The running coupling constant in QCD is expected to be strong enough on length scales $\sim 0.2–1$ fm to produce strong binding between quarks and to lead to dynamically hidden chiral symmetry. The confining forces are expected to operate on scales $\gtrsim 1$ fm and so have little effect on low-lying bound states. The σ meson and pions are introduced to describe the bound states in the channels in which the gluonic forces between quarks and antiquarks are most attractive, as well as the resulting hidden symmetry.

The Lagrangian density for the model is

$$\begin{aligned} \mathcal{L}(x) = & \bar{\psi}(x) \{ i\gamma \cdot \partial + g[\sigma(x) + i\tau \cdot \phi(x)\gamma_5] \} \psi(x) \\ & + \frac{1}{2} \partial_\mu \sigma(x) \partial^\mu \sigma(x) + \frac{1}{2} \partial_\mu \phi(x) \cdot \partial^\mu \phi(x) \\ & - \frac{\lambda^2}{4} [\sigma(x)^2 + \phi(x)^2 - v^2]^2 - F_\pi m_\pi^2 \sigma(x). \end{aligned} \quad (1.4)$$

The coupling between the quarks and mesons is chirally symmetric, as is the quartic "Mexican hat" potential for the mesons. The classical minimum of this potential occurs for a nonzero value of the σ field, $-F_\pi$, where $F_\pi = 93$ MeV is the pion decay constant. The final term in (1.4) is introduced to explicitly break the symmetry and give the pions their observed mass, $m_\pi = 139.6$ MeV.

In this model the quarks have a finite dynamical mass, $M_q = gF_\pi$. This is plausibly identified with the constituent-quark mass,^{36–38} which is believed to be about 300–500 MeV. Since the model has no confining force, free-quark states can appear. This should not be a problem for the ground-state baryon, which is strongly bound in this model. However, the model cannot be used in its present form to describe excited states.

The other adjustable parameter is the σ -meson mass, $m_\sigma = (2\lambda^2 F_\pi^2 + m_\pi^2)^{1/2}$. On the basis of the Nambu–Jona-Lasinio (NJL) model,³⁹ m_σ is expected to be of the order of twice M_q . In the MFA to the chiral model,⁸ reasonable agreement with observed nucleon properties was obtained for $M_q = 500$ MeV and $m_\sigma = 1200$ MeV. This value for m_σ is consistent with the observed $\epsilon(1300)$ resonance, which is plausibly identified with the σ meson

of the model.

In Sec. II the definition and basic properties of a coherent state are reviewed. The wave function for the hedgehog state is introduced in Sec. III, and its relation to the MFA is displayed. The projection onto spin-isospin eigenstates is given in Sec. IV. Details of the evaluation of matrix elements between these states can be found in the Appendix. Variation of the projected wave functions is described in Sec. V and the resulting nucleon properties are presented in Sec. VI. In Sec. VII the results are compared with the cloudy bag and Skyrme models. Section VIII contains a brief summary and outlines possible improvements on the present calculations.

II. THE COHERENT STATE

Before presenting the full hedgehog baryon state, I review the definition and basic properties of the coherent state^{21,26-29} for a single real scalar field. Such states are used here for the parts of the baryon wave function describing the σ field and each of the components of the pion field. In the general discussion, the generic scalar field will be denoted by σ .

The approximations to be used here are most easily obtained in the Hamiltonian formulation of the field theory. All operators are in the Schrödinger picture and so are time independent.

A general Fock-space representation of the field theory is obtained by expanding σ and its conjugate momentum as

$$\sigma(\mathbf{r}) = \sum_n \frac{1}{\sqrt{2\omega_n}} (a_n + a_n^\dagger) \phi_n(\mathbf{r}), \quad (2.1)$$

$$\pi(\mathbf{r}) = -i \sum_n \left[\frac{\omega_n}{2} \right]^{1/2} (a_n - a_n^\dagger) \phi_n(\mathbf{r}), \quad (2.2)$$

where, for the moment, the $\phi_n(\mathbf{r})$ are any complete set of normalized real functions and the frequencies, ω_n , are arbitrary, nonzero numbers. The "vacuum" state for this basis is defined by

$$a_n |0\rangle = 0 \quad \text{for all } n, \quad (2.3)$$

and can be regarded as an infinite-dimensional Gaussian wave packet whose principal axes are specified by the functions $\phi_n(\mathbf{r})$, and whose widths are inversely proportional to the corresponding $\sqrt{\omega_n}$.

A coherent state is defined by translating this wave packet in function space, so that it is centered on some nonzero field configuration, say, $F(\mathbf{r})$:

$$|F\rangle = N \exp \left[-i \int d^3r F(\mathbf{r}) \pi(\mathbf{r}) \right] |0\rangle. \quad (2.4)$$

The expectation value of $\sigma(\mathbf{r})$ in this state is just $F(\mathbf{r})$. It is convenient to work with an un-normalized state, and to rewrite (2.4) in the more familiar form

$$|F\rangle = e^{A^\dagger} |0\rangle, \quad (2.5)$$

where the (un-normalized) creation operator A^\dagger is defined by

$$A^\dagger = \sum_n \left[\frac{\omega_n}{2} \right]^{1/2} f_n a_n^\dagger, \quad (2.6)$$

and the f_n are the expansion coefficients of $F(\mathbf{r})$ in terms of the $\phi_n(\mathbf{r})$.

The generator-coordinate method leads to states which are linear combinations of coherent states centered on different field configurations. To evaluate expectation values in the projected states, we need overlaps and matrix elements between different coherent states. The overlap of two such states, $|F\rangle$ and $|G\rangle$, is

$$\langle F | G \rangle = \exp \left[\sum_n \frac{\omega_n}{2} f_n g_n \right]. \quad (2.7)$$

Matrix elements of normal-ordered products of field operators can be written as

$$\langle F | : \sigma(\mathbf{r})^m : | G \rangle = \bar{\sigma}(\mathbf{r})^m \langle F | G \rangle, \quad (2.8a)$$

$$\langle F | : \pi(\mathbf{r})^m : | G \rangle = \bar{\pi}(\mathbf{r})^m \langle F | G \rangle, \quad (2.8b)$$

where

$$\bar{\sigma}(\mathbf{r}) = \frac{F(\mathbf{r}) + G(\mathbf{r})}{2}, \quad (2.9a)$$

$$\bar{\pi}(\mathbf{r}) = -i \sum_n \frac{\omega_k}{2} (g_n - f_n) \phi_n(\mathbf{r}). \quad (2.9b)$$

So far, the basis used to expand the field operators (2.2) and (2.3) has been left unspecified. In principle, if one were to solve a field theory exactly, the results would not depend on the choice of basis. However, in the coherent-state approximation, the basis defines the fluctuation structure of the trial state, via (2.5) and (2.6). Hence results will be basis dependent.

The simplest choice of basis is the one which diagonalizes the noninteracting part of the Hamiltonian for small oscillations about the classical vacuum field configuration. In the MFA, the classical vacuum is assumed to approximate the expectation values of the fields in the true vacuum. Hence the basis for small fluctuations about this approximate vacuum seems to be the most appropriate, if one sticks closely to the spirit of the MFA; it will be used in the present work. In this basis, normal ordering a product of field operators corresponds to subtracting off its expectation value in the physical vacuum.

The creation operators for the σ field will be denoted by $a_0^\dagger(\mathbf{k})$, those for the pion field by $a_\alpha^\dagger(\mathbf{k})$, $\alpha=1,2,3$. The corresponding frequencies in the free-field basis are $\omega_{\sigma k} = (m_\sigma^2 + k^2)^{1/2}$ and $\omega_{\pi k} = (m_\pi^2 + k^2)^{1/2}$.

The use of the plane-wave basis means that the vacuum is both translationally and rotationally invariant. The translational invariance is unimportant for the present calculations but it will lead to substantial simplifications in the projection onto momentum eigenstates and the calculation of center-of-mass corrections, as in Ref. 21(a). The evaluation of matrix elements and overlaps in the projected states is simplified by the invariance of the basis under spatial and isospin rotations.

It is possible to improve on this approximation and still use a coherent state. For example, the one-loop⁴⁰ and Hartree approximations⁴¹ treat the fluctuations as in-

dependent modes, and so lead to Gaussian trial wave functions. In the one-loop case, the fields are expanded in terms of the normal modes for small oscillations about the soliton, rather than about the vacuum. The Hartree approximation corresponds to the use of the most general Gaussian trial function:⁴¹ both the modes and the corresponding frequencies are determined variationally. Both of these approaches are considerably more involved than the calculations presented here. They require renormalization and lead to highly nonlocal integral equations for the mean fields in solitons. In addition, the projection procedure will be complicated by the need to evaluate overlaps between "vacuum" states defined for the expansion bases about differently oriented solitons. Some steps toward extending this method to include distortion effects can be found in Ref. 21(b).

The quark field is expanded in a basis which includes distortion of the orbitals. The corresponding vacuum is thus not rotationally invariant. However, as in the MFA, the effects of this are neglected. This is consistent with the neglect of contributions of the distorted quark sea to the energy (full one-loop diagrams). For more discussion of one-loop effects, see the end of Sec. III.

III. THE HEDGEHOG BARYON

I now turn to the construction of the trial wave function for the hedgehog baryon. In principle, one would like to avoid the use of this ansatz and work directly with eigenstates of spin and isospin. The isovector, pseudoscalar nature of the pion makes this difficult. For example, a possible generalization of the coherent state is⁴²

$$|N\rangle = \exp \left[\sum_{\alpha, i} A_{\alpha i}^\dagger T_\alpha J_i \right] |3q\rangle, \quad (3.1)$$

where the $A_{\alpha i}^\dagger$ are creation operators for the nine components of an isovector, p -wave mode of the pion field, and \mathbf{T} and \mathbf{J} are the total quark isospin and angular momentum operators, respectively. If the bare three-quark state $|3q\rangle$ is a spin-isospin eigenstate then so is the state $|N\rangle$. However, as noted by Bolsterli,⁴² the algebra associated with states of the form (3.1) is exceedingly complicated. An alternative approach is to neglect components in the wave function with two or more pions. In the one-pion approximation it is then simple to ensure that states are coupled to good spin and isospin.⁴³

Here I will follow the approach used in the MFA and introduce the hedgehog ansatz. The coherent state constructed with this ansatz provides a quantum description of the mesonic part of the baryon wave function. It includes multipion components in a tractable way. It also tests earlier calculations, based on the MFA, which used an approximate projection method.⁸

The full hedgehog trial state is of the form

$$|H\rangle = e^{A_\sigma^\dagger} e^{A_h^\dagger} b_1^\dagger b_2^\dagger b_3^\dagger |0\rangle. \quad (3.2)$$

The b_i^\dagger 's create three quarks in the same space-spin-isospin state. They have different color quantum numbers in order to satisfy the Pauli principle. The quark state is a nodeless s -wave valence orbital:

$$q(\mathbf{r}) = \frac{1}{\sqrt{4\pi}} \begin{bmatrix} u(r)\chi_h \\ i\boldsymbol{\sigma} \cdot \hat{\mathbf{r}}v(r)\chi_h \end{bmatrix}, \quad (3.3)$$

where the spin and isospin are correlated in the spinor

$$\chi_h = \frac{1}{\sqrt{2}}(\chi_u\chi_d - \chi_d\chi_u). \quad (3.4)$$

This spinor satisfies the condition

$$(\boldsymbol{\sigma} + \boldsymbol{\tau})\chi_h = 0. \quad (3.5)$$

The pion coherent state is constructed using a p -wave creation operator with a similar correlation:

$$A_h^\dagger = i \int d^3k \left[\frac{\omega_{\pi k}}{2} \right]^{1/2} \tilde{h}(k) \hat{\mathbf{k}} \cdot \mathbf{a}^\dagger(\mathbf{k}). \quad (3.6)$$

An s -wave coherent state is used for the σ wave function. This is constructed with the creation operator

$$A_\sigma^\dagger = \int d^3k \left[\frac{\omega_{\sigma k}}{2} \right]^{1/2} \tilde{F}(k) a_0^\dagger(\mathbf{k}). \quad (3.7)$$

The correlations in (3.5) and (3.6) mean that the hedgehog baryon is a mixture of states with equal total spin and isospin:

$$|H\rangle = \sum_{JMM_T} (-1)^{J+M} C_J \delta_{M, -M_T} |JMM_T\rangle, \quad (3.8)$$

where $|JMM_T\rangle$ denotes an eigenstate with $T=J$. The hedgehog is analogous to the deformed states obtained in Hartree-Fock calculations for nuclei.²⁰ It should be a useful ansatz to the extent that the energy differences between the states in (3.8) (mainly N and Δ) can be regarded as small compared with single-particle excitation energies. Fiolhais, Urbano, and Goeke,⁴⁴ have shown that the hedgehog configuration minimizes the energy of a system of quarks and non-self-interacting pions in the mean-field (or coherent-state) approximation. This correlation between spin and isospin also occurs in the intrinsic wave functions of static-source models with strong coupling.^{45,46}

The expectation values of the σ and pion fields in the state (3.2) are

$$\frac{\langle H | \sigma(\mathbf{r}) | H \rangle}{\langle H | H \rangle} = -F_\pi + F(r) \equiv \sigma_0(r), \quad (3.9)$$

$$\frac{\langle H | \boldsymbol{\phi}(\mathbf{r}) | H \rangle}{\langle H | H \rangle} = \hat{\mathbf{r}}h(r), \quad (3.10)$$

where the radial functions $F(r)$ and $h(r)$ are the inverse Fourier transforms of the functions used to define the modes (3.6) and (3.7).

The model Hamiltonian, corresponding to (1.4), is

$$H = \int d^3r \left\{ \psi^\dagger(\mathbf{r}) \{ -i\boldsymbol{\alpha} \cdot \nabla - g\beta[\sigma(\mathbf{r}) + i\boldsymbol{\tau} \cdot \boldsymbol{\phi}(\mathbf{r})\boldsymbol{\gamma}_5] \} \psi(\mathbf{r}) + \frac{1}{2} [\pi_0(\mathbf{r})^2 + |\nabla\sigma(\mathbf{r})|^2 + |\boldsymbol{\pi}(\mathbf{r})|^2 + |\nabla\boldsymbol{\phi}(\mathbf{r})|^2] + \frac{\lambda^2}{4} [\sigma(\mathbf{r})^2 + \boldsymbol{\phi}(\mathbf{r})^2 - v^2]^2 + F_\pi m_\pi^2 \sigma(\mathbf{r}) - U_0 \right\}, \quad (3.11)$$

where the constant

$$U_0 = -\frac{m_\pi^2}{4\lambda^2} + F_\pi^2 m_\pi^2 \quad (3.12)$$

ensures that the energy density vanishes in the vacuum. With the approximations described above, the energy of the hedgehog baryon is just the expectation value of the normal-ordered Hamiltonian in (3.2). This can be evaluated with the help of the coherent-state properties to give

$$E = 4\pi \int r^2 dr \left\{ \frac{3}{4\pi} \left[u \frac{\partial v}{\partial r} - v \frac{\partial u}{\partial r} + \frac{2uv}{r} - g\sigma_0(u^2 - v^2) - 2ghuv \right] + \frac{1}{2} \left[\left(\frac{\partial \sigma_0}{\partial r} \right)^2 + \left(\frac{\partial h}{\partial r} \right)^2 + \frac{2}{r^2} h^2 \right] + \frac{\lambda^2}{4} (\sigma_0^2 + h^2 - v^2)^2 + F_\pi m_\pi^2 \sigma_0 - U_0 \right\}, \quad (3.13)$$

where $u(r)$ and $v(r)$ are the components of the quark function (3.3), $\sigma_0(r)$ and $h(r)$ are the mean fields defined in (3.9) and (3.10). The expression (3.13) is identical to the energy of the MFA (Refs. 8 and 9). Variation with respect to $u(r)$, $v(r)$, $F(r)$, and $h(r)$ yields the same dynamical equations as the semiclassical approximation to the Euler-Lagrange equations obtained from (1.4). Normal ordering subtracts off the (divergent) energy of the vacuum, $|0\rangle$, in the coherent-state approximation. Since the quantum fluctuations in the state (3.2) are the same as those in the vacuum, this leaves an energy which depends only on the mean fields in the soliton and not on the fluctuations about them.

The fact that the coherent state provides a complete wave function means that it is now possible to calculate quantities which were unobtainable in the MFA. In particular, the average numbers of σ mesons and pions are given by

$$\bar{N}_\sigma = 2\pi \int k^2 \omega_{\sigma k} \tilde{F}(k)^2 dk, \quad (3.14)$$

$$\bar{N}_\pi = 2\pi \int k^2 \omega_{\pi k} \tilde{h}(k)^2 dk. \quad (3.15)$$

These numbers can be calculated from the MFA solutions obtained in Ref. 8. The results, for the parameters $m_\sigma = 1200$ MeV and $M_q = 500$ MeV, are $\bar{N}_\sigma = 1.85$ and $\bar{N}_\pi = 1.18$.

Note that the MFA is not a zero-quantum approximation, as it is sometimes described. Fluctuations about the mean field must be present, by the uncertainty principle. The approximation is to neglect the effects of these on the dynamics of the system (loop diagrams). The fluctuations still can give nonzero expectation values to the meson number operators, as well as contributing to the total momentum and angular momentum [cf. Eq. (1.2)]. Note that these properties (3.14) and (3.15) depend on the functions and frequencies used in the expansion of the field

operators, as well as on the mean fields. Hence they cannot be calculated in the MFA without additional assumptions about the normal modes of the system.

The projection method used to calculate nucleon properties in Ref. 8 assumed that the pions did not contribute to the total spin and isospin; hence it cannot be exact. In the present work, I use a projection method based on the coherent state. This takes into account the angular momentum and isospin of the pion quanta.

The MFA also neglects contributions to the energy from the quark Dirac sea of negative-energy orbitals. The nodeless s -wave orbitals (3.3) can, for certain values of the model parameters, become bound to negative energies.^{8,47} It is still convenient to classify these orbitals as valence orbitals, since the occupation of these levels by quarks gives the system its baryon number of one. Also, as the parameters are varied, there is no discontinuous change in the properties of the baryon state at the point where these orbitals pass through zero energy.⁴⁸ If $M_q R$ is large enough (where R is the soliton radius) then "vacuum polarization" of the negative-energy continuum leads to a baryon-number density which is more diffuse than that obtained from the orbitals (3.3) alone.⁴⁷ In the limit $M_q R \gg 1$ (in practice⁴⁷ for $M_q R > 2.5$) the method of Goldstone and Wilczek⁴⁹ can be used to calculate this density in terms of derivatives of the pion fields. This approach leads to an expression for the baryon-number density which is identical to the topological charge density in the Skyrme model.¹³ The solitons studied here and in Ref. 8 have $M_q R \sim 1-2$, and so vacuum polarization effects are likely to be significant, although the calculations of Ripka and Kahana^{47,50} indicate that the qualitative features of the soliton should not be affected.

IV. PROJECTION

The hedgehog baryon defined in the previous section is not an eigenstate of spin or momentum. Eigenstates are obtained from it using Peierls-Yoccoz projection,²⁵ by analogy with the treatment of deformed nuclei.²⁰ The projected states are constructed in the "collective subspace"²⁴ spanned by all states of the form $\hat{R}(\Omega) |H\rangle$, where $\hat{R}(\Omega)$ is a spatial rotation through Euler angles Ω (Ref. 51). The appropriate weight functions for angular momentum projection are the D functions; the spin-isospin eigenstates are thus

$$|JMM_T\rangle = N_{JM_T} \int d^3\Omega D_{M,-M_T}^J(\Omega) \hat{R}(\Omega) |H\rangle. \quad (4.1)$$

The third component of the isospin, M_T , plays a role analogous to the band quantum number in a deformed nucleus.²⁰

The correlations in the hedgehog mean that it is invariant under combined spin and isospin rotations:

$$(\mathbf{J} + \mathbf{T}) |H\rangle = 0. \quad (4.2)$$

Hence separate projections for spin and isospin are not necessary. Other authors^{31,44} have suggested the use of more general coherent states without this property. These would include admixtures of states with $T \neq J$. Since $T \neq J$ resonances generally lie well above the nucleon in

energy, such admixtures are likely to be small in intrinsic states corresponding to the N and Δ .

It is simplest to work only with states for which $M = -M_T$, since these can be obtained from the hedgehog with the projection operators

$$P_{JM} = \frac{2J+1}{8\pi^2} \int d^3\Omega D_{M,M}^J(\Omega) \hat{R}(\Omega). \quad (4.3)$$

These have the basic properties of projection operators, namely,

$$(P_{JM})^\dagger = P_{JM}, \quad (4.4a)$$

$$(P_{JM})^2 = P_{JM}. \quad (4.4b)$$

If the projected states are normalized to unity, then (4.1)–(4.4) can be used to obtain an expression for the N_{JM_T} :

$$\begin{aligned} N_{J-M}^2 &= \left[\frac{2J+1}{8\pi^2} \right]^2 (\langle H | P_{JM} | H \rangle)^{-1} \\ &= \frac{2J+1}{8\pi^2} \left[\int d^3\Omega D_{M,M}^J(\Omega) \langle H | \hat{R}(\Omega)^{-1} | H \rangle \right]^{-1}. \end{aligned} \quad (4.5)$$

The coefficients C_J in the expansion (3.8) are given by

$$\begin{aligned} C_J^2 &= \langle H | P_{JM} | H \rangle \\ &= \frac{2J+1}{8\pi^2} \int d^3\Omega D_{M,M}^J(\Omega) \langle H | \hat{R}(\Omega)^{-1} | H \rangle. \end{aligned} \quad (4.6)$$

The probability of finding a state of spin J in the

$$P_{JM} V_{1m} P_{JM} = \frac{2J+1}{8\pi^2} \langle JM 1m | JM \rangle \sum_{M'm'} \langle JM 1m' | JM' \rangle \int d^3\Omega D_{M',M}^J(\Omega) \hat{R}(\Omega)^{-1} V_{1m'}. \quad (4.12)$$

Hence the expectation value of V_3 in the state $|JM - M\rangle$ can be written as

$$\langle JM - M | V_3 | JM - M \rangle = \langle JM 10 | JM \rangle \sum_{M'm} \langle JM 1m | JM' \rangle \frac{\int d^3\Omega D_{M',M}^J(\Omega) \langle H | \hat{R}(\Omega)^{-1} V_{1m} | H \rangle}{\int d^3\Omega D_{M',M}^J(\Omega) \langle H | \hat{R}(\Omega)^{-1} | H \rangle}. \quad (4.13)$$

The Appendix contains details of the evaluation of (4.11) and (4.13) for various operators corresponding to terms in the energies and other properties of baryons. It is straightforward to generalize these results to include transition matrix elements between states of different J , although I have not done so here.

The energy of the projected state with spin J is

$$\begin{aligned} E_J &= \langle JMM_T | :H: | JMM_T \rangle \\ &= 4\pi \int r^2 dr \left\{ \frac{3}{4\pi} \left[u \frac{\partial v}{\partial r} - v \frac{\partial u}{\partial r} + \frac{2uv}{r} - g\sigma_0(u^2 - v^2) - 2ghuv \right] + \frac{1}{2} \left[\frac{\partial \sigma_0}{\partial r} \right]^2 \right. \\ &\quad + \frac{1}{2} \left[\left[\frac{\partial h}{\partial r} \right]^2 + \frac{2}{r^2} h^2 + m_\pi^2 h^2 \right] C_0(J; \bar{N}_\pi) + \frac{\lambda^2}{4} (\sigma_0^2 - v^2)^2 + \frac{\lambda^2}{2} (\sigma_0^2 - F_\pi^2) h^2 C_2(J; \bar{N}_\pi) \\ &\quad \left. + \frac{\lambda^2}{4} h^4 C_4(J; \bar{N}_\pi) + F_\pi m_\pi^2 \sigma_0 - U_0 \right\}. \end{aligned} \quad (4.14)$$

hedgehog is related to C_J by

$$P_J = \frac{(2J+1)C_J^2}{\langle H | H \rangle}, \quad (4.7)$$

where

$$\langle H | H \rangle = e^{\bar{N}_\sigma + \bar{N}_\pi}. \quad (4.8)$$

The expectation value of a scalar operator S in one of the projected states is

$$\begin{aligned} \langle JM - M | S | JM - M \rangle \\ = \left[\frac{8\pi^2}{2J+1} \right]^2 N_{J-M}^2 \langle H | P_{JM} S P_{JM} | H \rangle. \end{aligned} \quad (4.9)$$

This can be simplified, since S commutes with the rotation operators, and hence with P_{JM} . Using this, along with (4.3) and (4.5), the matrix element can be written as a ratio of two angular integrals:

$$\begin{aligned} \langle JM - M | S | JM - M \rangle \\ = \frac{\int d^3\Omega D_{M,M}^J(\Omega) \langle H | \hat{R}(\Omega)^{-1} S | H \rangle}{\int d^3\Omega D_{M,M}^J(\Omega) \langle H | \hat{R}(\Omega)^{-1} | H \rangle}. \end{aligned} \quad (4.10)$$

Similar manipulations can be performed on the matrix elements of vector operators. These operators transform under rotations as

$$\hat{R}(\Omega)^{-1} V_{1m} \hat{R}(\Omega) = \sum_{m'} D_{m,m'}^1(\Omega) V_{1m'}, \quad (4.11)$$

and so do not commute with P_{JM} . Using (4.11), the definition (4.3), and recoupling the D functions gives

This differs from the unprojected energy (3.13) because of the projection coefficients $C_i(J; \bar{N}_\pi)$. These depend on the spin of the state and on the average number of pions in the unprojected state (3.15). Their full forms are given in the Appendix.

Since the σ mesons are isoscalar and in s waves, their average number is unchanged by projection. The number of pions in the projected state is related to \bar{N}_π by

$$\langle N_\pi \rangle_J = \bar{N}_\pi C_0(J; \bar{N}_\pi). \quad (4.15)$$

Table I gives the energies and average numbers of pions for projected states obtained from the MFA field distributions⁸ for the parameters $m_\sigma = 1200$ MeV and $M_q = 500$ MeV. Also listed are the probabilities of finding each of the states with good spin in the unprojected hedgehog. The largest probabilities are those for states with $J \leq \frac{5}{2}$. The Δ lies ~ 120 MeV above the nucleon, and a $J = \frac{5}{2}$ is ~ 300 MeV higher still. However, these energies should not be taken too seriously, since they have been obtained by variation before projection. In the next section I discuss the better procedure of variation after projection. The average number of pions increases with J ; at least one pion is needed to form a state with $J = \frac{5}{2}$, at least two for $J = \frac{7}{2}$, etc.

The energies of the states with $J > \frac{5}{2}$ increase rapidly with J . These states are very small components of the unprojected wave function and so should be regarded as artifacts of the approximations.

Finally, the numbers of Table I provide several numerical checks on the calculations: the probabilities P_J add up to one, as they should; the averages of the E_J and the $\langle N_\pi \rangle_J$, weighted with these probabilities, reproduce the energy (1119 MeV) and number of pions (1.18) for the unprojected state.

V. VARIATION AFTER PROJECTION

The numbers presented in Table I are obtained by varying the field functions to obtain a stationary value for the energy of the hedgehog, (3.13), and then projecting. A better procedure is to look for stationary values of the energies of the projected states, (4.14), since it is these states

TABLE I. Decomposition of the hedgehog wave function in terms of eigenstates of spin and isospin. The wave function is constructed with the fields obtained from a MFA calculation, for the parameters $M_q = 500$ MeV and $m_\sigma = 1200$ MeV.

J	P_J	E_J (MeV)	$\langle N_\pi \rangle_J$
$\frac{1}{2}$	0.293	924	0.70
$\frac{3}{2}$	0.452	1041	1.02
$\frac{5}{2}$	0.200	1355	1.80
$\frac{7}{2}$	0.047	1839	2.69
$\geq \frac{9}{2}$	< 0.01		

that are to be treated as approximate eigenstates of the Hamiltonian. Note that the spectrum of the Dirac equation is unbounded from below, and so the "best" value for the energy is only a stationary point, not a minimum with respect to all variations.

Variations of (4.14) with respect to $u(r)$, $v(r)$, and $\sigma_0(r)$ lead to the coupled equations

$$\frac{\partial u}{\partial r} + (\epsilon - g\sigma_0)v + ghv = 0, \quad (5.1a)$$

$$\frac{\partial v}{\partial r} + \frac{2v}{r} - (\epsilon + g\sigma_0)u - ghv = 0, \quad (5.1b)$$

$$-\frac{\partial^2 \sigma_0}{\partial r^2} - \frac{2}{r} \frac{\partial \sigma_0}{\partial r} - g(u^2 - v^2) + \lambda^2(\sigma_0 - v^2)\sigma_0 + F_\pi m_\pi^2 + \lambda^2 \sigma_0 h^2 C_2(J; \bar{N}_\pi) = 0, \quad (5.1c)$$

where ϵ is the Lagrange multiplier for the quark normalization condition:

$$\int r^2(u^2 + v^2)dr = 1. \quad (5.2)$$

These nonlinear differential equations are similar in form to the MFA equations, except for the presence of the projection coefficients. Through their dependence on \bar{N}_π , these coefficients are functions of the pion field $h(r)$. Their appearance in (4.14) leads to a nonlinear integrodifferential equation when the energy is varied with respect to $h(r)$:

$$\left[-\frac{\partial^2 h}{\partial r^2} - \frac{2}{r} \frac{\partial h}{\partial r} + \frac{2}{r^2} h + m_\pi^2 h \right] C_0(J; \bar{N}_\pi) + \lambda^2(\sigma_0^2 - F_\pi^2) h C_2(J; \bar{N}_\pi) + \lambda^2 h^3 C_4(J; \bar{N}_\pi) - \frac{6}{4\pi} guv + h_\omega(r) \frac{\partial E_J}{\partial \bar{N}_\pi} = 0, \quad (5.3)$$

where

$$\frac{\partial E_J}{\partial \bar{N}_\pi} = 4\pi \int r^2 dr \left\{ \frac{1}{2} \left[\left(\frac{\partial h}{\partial r} \right)^2 + \frac{2}{r^2} h^2 + m_\pi^2 h^2 \right] \frac{dC_0(J; \bar{N}_\pi)}{d\bar{N}_\pi} + \frac{\lambda^2}{2} (\sigma_0^2 - F_\pi^2) h^2 \frac{dC_2(J; \bar{N}_\pi)}{d\bar{N}_\pi} + \frac{\lambda^2}{4} h^4 \frac{dC_4(J; \bar{N}_\pi)}{d\bar{N}_\pi} \right\}, \quad (5.4)$$

and $h_\omega(r)$ is defined by

$$h_\omega(r) = \frac{1}{4\pi r^2} \frac{\delta \bar{N}_\pi}{\delta h(r)} = \left[\frac{2}{\pi} \right]^{1/2} \int k^2 \omega_{\pi k} \tilde{h}(k) j_1(kr) dk. \quad (5.5)$$

The solutions to these equations should satisfy the

boundary conditions, for $r \rightarrow \infty$,

$$u(r) \sim \frac{1}{r} \exp[-(M_q^2 - \epsilon^2)^{1/2} r], \quad (5.6a)$$

$$\sigma_0(r) + F_\pi \sim \frac{1}{r} e^{-m_\sigma r}, \quad (5.6b)$$

$$h(r) \sim \frac{1}{r} e^{-m_\pi r}, \quad (5.6c)$$

as in the MFA.

Fortunately, the final term in (5.3) is relatively small for the range of parameters studied here. A simple iterative procedure is thus sufficient to solve the coupled equations (5.1) and (5.3). Initial forms are guessed for the functions $u(r)$, $v(r)$, $\sigma_0(r)$, and $h(r)$ —the MFA results⁸ provide a suitable starting point. These are used to calculate the $C_i(J; \bar{N}_\pi)$, $h_\omega(r)$, and $\partial E_J / \partial \bar{N}_\pi$, which are then kept fixed. The resulting coupled, nonlinear, differential equations are then solved using the package COLSYS (Ref. 52). The quark eigenvalue ϵ is iterated on until (5.2) is satisfied. The new field functions are then used to recalculate the $C_i(J; \bar{N}_\pi)$, $h_\omega(r)$, and $\partial E_J / \partial \bar{N}_\pi$, and the procedure is repeated until adequate convergence is achieved. The whole process takes ~ 20 – 25 min on a VAX 11/780. This time could be reduced by combining the iteration on ϵ with the main iteration, or by using the method of Köppel and Harvey,⁵³ which determines the coupling g at the end of the calculation.

The N and Δ energies and average numbers of pions are shown in Table II, for three values of M_q , all with $m_\sigma = 1200$ MeV. The energies decrease with increasing M_q because of the increase in the attractive quark-pion interaction. The dependence on m_σ is much weaker: the nucleon energy ranges from 828 to 919 MeV as m_σ is changed from 600 to 2000 MeV (with $M_q = 500$ MeV). This is similar to the results in the MFA (Ref. 8). Both the unprojected and projected wave functions are dominated by field configurations in which $\sigma(\mathbf{r})^2 + \phi(\mathbf{r})^2$ is close to F_π^2 . This can be seen from Fig. 1, which shows the functions $\sigma_0(r)$ and $h(r)$. These field configurations correspond to the peak, in function space, of the coherent-state wave packet. Since the fields lie close to the circular minimum of the Mexican hat potential [see (1.4)], the energy of the system is relatively insensitive to m_σ , which determines the curvature of the potential at the minimum. In general, the differences between variation before and after projection are relatively small, as can be seen from Figs. 1 and 2.

The N - Δ mass splitting is, in all cases, about half the observed 300 MeV. This may, in part, be due to the hedgehog ansatz, and the restrictions it imposes on the trial states used in variation after projection. It is also likely that additional spin-dependent interactions between the quarks are needed. These would correspond to residual gluonic interactions, which are not included in the collective effects modeled by the pions and σ meson. Similar interactions are needed in the cloudy bag model,³² in order to fit the N - Δ splitting.

The parameter set $M_q = 450$ MeV, $m_\sigma = 1200$ MeV

TABLE II. Dependence of M_q of the N and Δ energies obtained by variation after projection. Also shown are the average numbers of pions in these states. The σ mass was 1200 MeV in all cases. All energies and masses are in MeV.

M_q	E_N	$\langle N_\pi \rangle_N$	E_Δ	$\langle N_\pi \rangle_\Delta$
400	1108	0.82	1238	1.12
450	1000	0.89	1141	1.23
500	871	0.93	1023	1.31
550	726	0.96	891	1.37

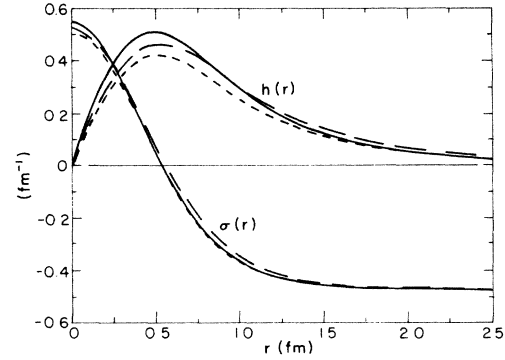


FIG. 1. Meson field distributions obtained by variation after projection. The solid lines are $\sigma_0(r)$ and $h(r)$ for the nucleon; the long-dashed lines are for the Δ . For comparison, the unprojected MFA results (Ref. 8) are also shown, by the short-dashed lines.

gives an average of the N and Δ masses which is in good agreement with its experimental value, 1080 MeV. This set will be used in the rest of this work.

The average numbers of pions in the N and Δ wave functions are close to one, while the average numbers of σ mesons are 1.7 and 1.9, respectively. Table III lists the probabilities $P(n\pi)$ of finding n pions in the projected baryon wave functions. These probabilities are calculated using matrix elements of the appropriate projection operators in (4.11). They show that the N and Δ wave functions contain significant two-pion components, in addition to those with zero and one pion.

As well as the N and Δ states, a baryon state with $J = T = \frac{5}{2}$ is obtained by variation after projection. For the parameters $M_q = 500$ MeV, $m_\sigma = 1200$ MeV, this state lies at 390 MeV above the nucleon. No such state has been observed, although it would be experimentally difficult to detect, due to its isospin of $\frac{5}{2}$. The pionic content of this state is much larger than that in the N or Δ : its average number of pions is 2.4. Although this state is a significant component of the unprojected hedgehog (cf. Table I), it still may be an artifact of the approximations, and not a feature of the model. It lies above the $N\pi\pi$

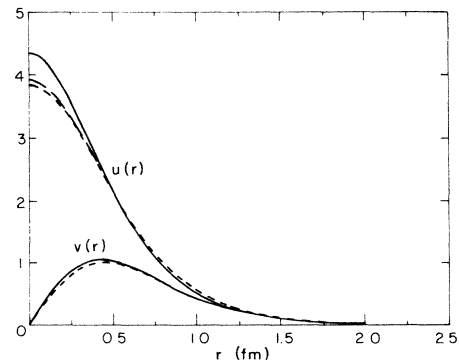


FIG. 2. Quark wave-function components, $u(r)$ and $v(r)$, obtained by variation after projection. For notation see Fig. 1.

TABLE III. Probabilities of finding n pions in the N and Δ wave functions. The results are for the parameters $M_q=450$ MeV, $m_\sigma=1200$ MeV.

n	$P_N(n\pi)$	$P_\Delta(n\pi)$
0	0.445	0.270
1	0.323	0.391
2	0.157	0.220
3	0.055	0.086
4	0.015	0.026
≥ 5	< 0.01	< 0.01

threshold, and so it is possible that coupling to the continuum would be so strong as to give no clear resonance.

VI. NUCLEON PROPERTIES

The wave functions can be used to calculate a variety of baryon properties, in addition to their energies. In this section, results for nucleon electromagnetic properties, axial coupling, and π - N coupling are presented. Also, I compare these results with those obtained in Ref. 8 by an approximate projection method.

Electromagnetic properties, such as magnetic moments and charge radii, are calculated by taking the appropriate moments of matrix elements of the electromagnetic current:

$$J_{EM}^\mu = \bar{\psi} \gamma^\mu \left(\frac{1}{6} + \frac{1}{2} \tau_3 \right) \psi + \epsilon_{3\alpha\beta} \phi_\alpha \partial^\mu \phi_\beta. \quad (6.1)$$

The axial coupling constant, measured in neutron β decay, is a matrix element of the space part of the isovector axial-vector current:

$$A^\mu = \frac{1}{2} \bar{\psi} \gamma^\mu \gamma_5 \tau \psi + \sigma \partial^\mu \phi - \phi \partial^\mu \sigma. \quad (6.2)$$

The π - N coupling constant can be calculated in two ways: as a matrix element either of the pion field ϕ or of the pion-source current

$$\begin{aligned} \mathbf{j}_\pi &= (\square + m_\pi^2) \phi \\ &= ig \bar{\psi} \gamma_5 \tau \psi - \lambda^2 (\sigma^2 + \phi^2 - F_\pi^2) \phi. \end{aligned} \quad (6.3)$$

Finally, the σ commutator, extracted from s -wave π - N scattering,^{54,55} is given by the matrix element of the explicit symmetry-breaking term in the Hamiltonian (3.11):

$$H_{sb} = F_\pi m_\pi^2 \int d^3r [\sigma(\mathbf{r}) + F_\pi]. \quad (6.4)$$

These properties should be evaluated by taking matrix elements between nucleon momentum eigenstates. In a coherent-state treatment, such states can be constructed from the localized soliton by using Peierls-Yoccoz projection.²⁵ This procedure has been carried out in Ref. 21 for the soliton bag model. It will be more complicated in the model studied here, due to the need for projection onto eigenstates of both angular and linear momentum. In the present work, I follow the approach used in bag models⁵⁶ (and in Ref. 8) and interpret the localized state as a nucleon wave packet. Nucleon properties are then evaluated assuming that the momenta in the packet are small enough to be treated as nonrelativistic.

With the above assumptions, the proton magnetic mo-

ment is given by

$$\mu_p = \frac{1}{2} \langle p \uparrow | \int d^3r [\mathbf{r} \times \mathbf{J}_{EM}(\mathbf{r})]_z | p \uparrow \rangle, \quad (6.5)$$

and its mean-square charge radius by

$$r_p^2 = \langle p \uparrow | \int d^3r r^2 J_{EM}^0(\mathbf{r}) | p \uparrow \rangle. \quad (6.6)$$

The axial coupling is

$$g_A = 2 \langle p \uparrow | \int d^3r A_3^z(\mathbf{r}) | p \uparrow \rangle. \quad (6.7)$$

As a matrix element of the pion field, the π - N coupling is

$$\frac{g_{\pi NN}}{2M} = m_\pi^2 \langle n \uparrow | \int d^3r z \phi_3(\mathbf{r}) | n \uparrow \rangle, \quad (6.8)$$

while the alternative expression, in terms of the pion-source current, is

$$\frac{g_{\pi NN}}{2M} = \langle n \uparrow | \int d^3r z j_{\pi 3}(\mathbf{r}) | n \uparrow \rangle. \quad (6.9)$$

The σ commutator is defined by

$$\sigma_{\pi N} = \langle p \uparrow | \int d^3r [\sigma(\mathbf{r}) + F_\pi] | p \uparrow \rangle. \quad (6.10)$$

Details of the evaluations of these matrix elements can be found in the Appendix. The numerical results are displayed in Table IV. In general, the agreement with experiment is reasonable. The major differences are for g_A/g_V and $\sigma_{\pi N}$, but Broniowski and Banerjee¹⁰ have shown that the extension of this model to include vector mesons leads to a significant improvement in these numbers. The π - N coupling is also significantly larger than its observed value. However, this is not an entirely independent quantity since, in a self-consistent solution to the model, $g_{\pi NN}$ and g_A are related by the Goldberger-Treiman relation.

As noted in Ref. 8, g_A and $\sigma_{\pi N}$ are the only observables which depend directly on the σ field. The large meson piece of g_A in this model is due to the large deviation of the mean σ field from its vacuum value, $-F_\pi$ (see Fig. 1). In the cloudy bag model,³² there is no such mesonic contribution, at least to lowest order, since the σ field is essentially fixed to its vacuum value. The model of Ref. 10 uses a smaller value for the quark-scalar-meson coupling g . This leads to a mean σ field with a radius ~ 0.4 fm, as compared to ~ 0.6 fm in the model without vector mesons. The meson pieces of g_A and $\sigma_{\pi N}$ are correspondingly less. The smaller value for g also leads to a smaller $g_{\pi NN}$, as required by the Goldberger-Treiman relation. It should be noted that the inclusion of vacuum polarization effects may also tend to reduce the σ radius, and weaken the effective quark-pion coupling.⁵⁰

For comparison, Table IV also contains the results of Ref. 8. The quark pieces of these were calculated neglecting the meson contributions to the total spin and isospin of the nucleon. The meson pieces were obtained in a coherent-state-type approximation, which is identical to the present method for operators linear in the pion field (see the Appendix). In general, the present results are somewhat smaller than those of Ref. 8. There is little difference in the meson pieces, but the quark pieces are re-

TABLE IV. Nucleon properties. Those shown are the proton and neutron magnetic moments (in nuclear magnetons n.m.) and mean-square charge radii, the axial-vector coupling and its mean-square radius, the π - N coupling constant, calculated using Eqs. (6.8) and (6.9), and the mean-square radius of the pion source, the σ commutator, and the mean-square radius of the quark density. Where relevant, quark and meson contributions to the properties have been separated. The parameter set used is $M_q = 450$ MeV, $m_\sigma = 1200$ MeV. The numbers in parentheses are the results of the MFA calculations of Ref. 8 (with numerical errors corrected as in Ref. 10), for $M_q = 500$ MeV.

	Quark	Meson	Total	Experiment	
μ_p (n.m.)	1.38	1.20	2.58	(2.87)	2.79
μ_n (n.m.)	-1.03	-1.20	-2.23	(-2.29)	-1.91
r_{Cp}^2 (fm ²)	0.39	0.16	0.55		0.70
r_{Cn}^2 (fm ²)	0.09	-0.16	-0.07		-0.12
g_A/g_V	0.98	0.81	1.78	(1.86)	1.26
r_A^2 (fm ²)	0.20	0.21	0.41	(0.42)	0.52±0.17
$\frac{m_\pi}{2M} g_{\pi NN}$ (6.8)			0.93	(1.06)	1.00
$\frac{m_\pi}{2M} g_{\pi NN}$ (6.9)	0.87	0.41	1.28	(1.53)	
r_π^2 (fm ²)	0.54	0.39	0.93	(0.85)	
$\sigma_{\pi N}$ (MeV)			86	(92)	35±10
r_q^2 (fm ²)			0.48	(0.47)	

duced by ~ 15 – 20 %. The reduction in the quark pieces is due to the quantum treatment of the pions. This allows mixing of various quark spin-isospin states into the nucleon wave function. For example, a spin-up proton is sometimes three quarks with the quantum numbers of a spin-down proton (or a neutron or a Δ) plus one or more pions. In the perturbative language of the cloudy bag model,³² the reduction of the quark piece would be described as a combination of wave-function and vertex renormalizations.

Another consequence of the quantum treatment of the pions is that they can carry electric charge, and hence they can contribute to the nucleon charge radii. The calculated values for these radii are in reasonable agreement with experiment.

Although the calculated proton magnetic moment is in good agreement with experiment, the ratio of proton and neutron moments is rather poor. The present results give $\mu_p/\mu_n = -1.16$. The experimental value is -1.46 , close to the pure quark model result of -1.5 . This suggests that the pionic component of the wave function obtained here is too large to be realistic. As well as contributing directly to the isovector moment, the pions reduce the quark pieces of the moments as described above. Both effects reduce the isoscalar moment relative to the isovector, and so bring μ_p/μ_n closer to -1 . Another constraint on the number of pions in the nucleon wave function is provided by the ratio of strange to nonstrange sea quarks observed in deep-inelastic scattering. Thomas⁵⁷ has used the results of deep-inelastic neutrino and antineutrino scattering to obtain an upper bound of about 0.5 pions per nucleon, although the uncertainties are rather large. On the other hand, the number of pions cannot be too small, as it is then difficult to get agreement with the nucleon charge radii.

The two calculations of the π - N coupling, (6.10) and (6.11), differ by about 35%. The difference between them corresponds to a virial theorem of the kind discussed in

Ref. 21. These virial theorems are time derivatives of expectation values of various operators. They should vanish for an exact eigenstate of the Hamiltonian. In the Schrödinger picture they can be evaluated in the form

$$i \frac{d}{dt} \langle O \rangle = \langle [O, H] \rangle. \quad (6.11)$$

The extent to which an approximate solution satisfies these virial theorems provides a test of the approximations used. Of course, their satisfaction is only a necessary, not sufficient, condition for an approximate solution to be a good one.

In the present case, the difference between (6.8) and (6.9) is the time derivative of the expectation value of

$$O = \int d^3r z \pi_3(\mathbf{r}), \quad (6.12)$$

where $\pi_3(\mathbf{r})$ is the conjugate momentum to $\phi_3(\mathbf{r})$. The corresponding Eq. (6.11) is an integral of the Euler-Lagrange equation for the pion field. The analogous virial theorem for the σ field is automatically satisfied, since it is a consequence of the variational equation (5.1c).

Another useful virial theorem is provided by the Goldberger-Treiman relation. This is obtained by considering

$$O = \int d^3r z A_3^0(\mathbf{r}). \quad (6.13)$$

From the PCAC (partial conservation of axial-vector current) equation

$$\partial_\mu \mathbf{A}^\mu = F_\pi m_\pi^2 \phi, \quad (6.14)$$

the vanishing of (6.9) in an exact eigenstate leads to the usual relation

$$g_A = \frac{F_\pi}{M} g_{\pi NN}, \quad (6.15)$$

where the couplings are both evaluated at zero three-momentum transfer, (6.7)–(6.9). The values for g_A calculated using (6.15) and the results of Eqs. (6.8) and (6.9) are

1.24 and 1.70, respectively. These are to be compared with the directly calculated value 1.78. The agreement between the number from (6.9) and g_A is very satisfactory. However, the 35% discrepancy between (6.8) and (6.9) is disturbing and suggests that the present calculations need to be improved on.

The experimental value of $g_{\pi NN}$ is obtained not at zero three-momentum transfer but at $\mathbf{q}^2 = -m_\pi^2$. For small \mathbf{q}^2 the difference between $g_{\pi NN}(\mathbf{q}^2)$ and $g_{\pi NN}(0)$ can be estimated from³²

$$g_{\pi NN}(\mathbf{q}^2) \simeq g_{\pi NN}(0) \left(1 - \frac{1}{6} r_\pi^2 \mathbf{q}^2\right), \quad (6.16)$$

where r_π^2 is the mean-square radius of the pion-source current:

$$r_\pi^2 = \frac{1}{g_{\pi NN}(0)} \left\langle n \uparrow \left| \int d^3r r^2 z j_{\pi 3}(\mathbf{r}) \right| n \uparrow \right\rangle, \quad (6.17)$$

where $g_{\pi NN}(0)$ is given by (6.9). The calculated r_π^2 corresponds to a value for $g_{\pi NN}(-m_\pi^2)$ which is 5% larger than $g_{\pi NN}(0)$. This is comparable with the $\sim 7\%$ discrepancy in the Goldberger-Treiman relation for the experimentally observed values of g_A and $g_{\pi NN}$.

VII. COMPARISONS WITH OTHER MODELS

It is interesting to compare the nucleon wave function obtained in the present approach with those used in other models. Here I consider two models which also include pionic degrees of freedom and (approximate) chiral symmetry: the cloudy bag model and the Skyrme model.

The cloudy bag model³² describes hadrons in terms of massless quarks confined inside a bag. To maintain axial-vector-current conservation, the quarks are coupled to the pion field at the surface of the bag (or through an equivalent pseudovector coupling in the bag interior). The pion field is described by a nonlinear σ model. For large bag radii (≥ 0.8 fm) the quark-pion coupling is weak enough for a perturbative treatment to be justified. The pion field can thus be quantized using the linearized approximation for small oscillations about the vacuum. This is in contrast with models with small bag radii,⁵⁸ where the pion coupling is too strong for perturbative methods to work.⁴⁶

Despite the differences in their physical motivations, the linear σ model studied here and the cloudy bag model lead to surprisingly similar nucleon wave functions. Both are in good agreement with observed nucleon electromagnetic quantities and both give quark wave functions with rms radii ~ 0.7 fm. If the pions are treated to first order in the cloudy bag model, the average number of pions in the nucleon wave function is between 0.3 and 0.5, for bag radii between 1.0 and 0.8 fm. When components with more than one pion are included, an upper bound of 0.9 pions is obtained, for a bag radius of 0.8 fm. This is comparable to the average number of pions per nucleon obtained in the present work, which includes multipion components via the coherent state. Deep-inelastic scattering results⁵⁷ suggest that a smaller number of pions may be more realistic, corresponding to bag radii of about 0.9 fm or larger.

Another approach, which has received much attention

recently, is the Skyrme model.¹³⁻¹⁶ By contrast with the model studied here and the cloudy bag, this model does not include explicit quark degrees of freedom. Instead it is based on a nonlinear σ model with a fourth-order derivative interaction (or coupling to vector mesons¹⁶) to produce stable solitons. These are known as "Skyrmions." The solitons with a winding number of one are identified with baryons, since topological arguments show that they can be quantized as fermions.^{59,60} The hedgehog ansatz is used, and the field distributions in the resulting solitons are qualitatively similar to those shown in Fig. 1, except that they satisfy the nonlinear constraint $\sigma^2 + \phi^2 = F_\pi^2$. In fact, a Lagrangian very similar to the one proposed by Skyrme can be obtained from the present model by integrating out the quark degrees of freedom. In the limit where the quark-meson coupling is large, the resulting effective Lagrangian can be expanded in powers of derivatives of the pion field and the leading terms include the Skyrme fourth-order interaction.⁶¹ In this large- g limit, the identification of the topological winding number with baryon number^{47,49} can be understood in terms of the deeply bound quark orbitals discussed in Sec. III.

As originally described, the Skyrmion is a hedgehog object. Before its properties can be compared with those of a real nucleon, some way must be found to quantize it and project out spin-isospin eigenstates. However, as noted in Sec. I, the nonlinear constraint on this model means that it cannot be quantized in the usual canonical way. Hence, for example, the methods of the present work cannot be applied to it. At present, there is no way to quantize all the model's degrees of freedom in a manner which can handle large-amplitude fluctuations, such as collective rotations of a Skyrmion. (Numerous authors⁶² have used linearized approximations for small-amplitude oscillations, to study vibrational excitations and π - N scattering in the Skyrme model.)

In lieu of a complete quantization, Adkins, Nappi, and Witten have proposed a semiclassical approach.¹⁴ This quantizes only the collective coordinates associated with rotations of the Skyrmion, treating it as a rigid rotor. It leads to a Hamiltonian which has a local dependence on the collective coordinates [the Euler angles describing the relative orientation of the spin and isospin axes in the hedgehog, cf. Eq. (4.1)]. Hence this approach implicitly assumes that the overlap between rotated and unrotated hedgehog states is essentially a δ function of the Euler angles:

$$\langle H | \hat{R}(\Omega)^{-1} | H \rangle \propto \delta^3(\Omega). \quad (7.1)$$

Such an assumption should be good in a situation where the nucleon wave function contains a large number of quanta. This would be the case in the limit where the number of colors is large⁶³ (a limit often used in motivation for the Skyrme model⁶⁰) or if the nucleon were a strongly coupled source for the pion field.⁶⁴ Neither of these cases corresponds to the real world with three colors and, at most, about one pion per nucleon. This is illustrated in Fig. 3, which shows the dependence of the overlap [see Eq. (A3)] on one of the Euler angles, for various numbers of quarks and pions. For the soliton studied here, the overlap has a width $\sim \pi/3$, which is not much

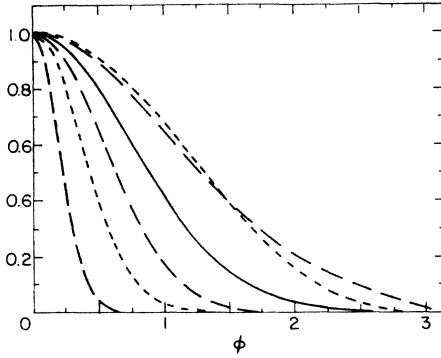


FIG. 3. Dependence of the overlap $\langle H | \hat{R}(\Omega)^{-1} | H \rangle$ on the Euler Φ $\{\cos \Phi/2 = \cos(\beta/2)\cos[(\alpha+\gamma)/2]\}$. The solid line corresponds to the soliton studied here, with $N_c=3$ quarks and $\bar{N}_\pi \simeq 1.5$ pions in the unprojected hedgehog. The long-dashed lines show the results for $N_c=1, 11$, and 101 , all with $\bar{N}_\pi=1$. The short-dashed lines are for $\bar{N}_\pi=0$ and 10 , both with $N_c=3$.

smaller than for a bare three-quark hedgehog.

Because of its assumption of a large number of quanta, this method predicts an infinite rotational band of $J=T$ baryon states. No such states have been observed for spin $\frac{5}{2}$ or greater. Also, it is difficult to obtain a better than qualitative description of nucleon properties in this approach. In particular, rather poor agreement with experiment is obtained when F_π is fixed to its measured value. A further problem is that the semiclassical quantization is not a projection method (such as the one used in this work). Hence "variation after projection" is dangerous: Braaten and Ralston⁶⁵ have shown that the Skyrmion tends to collapse if such a procedure is attempted. This is due to the fact that the semiclassical rotor can radiate pion waves unless the pion mass is larger than the frequency of rotation.

VIII. SUMMARY

The coherent state²⁶⁻²⁹ provides a full quantum description for the bosonic parts of soliton wave functions. It has many features of the mean-field approximation for localized states which break the translational, and other, symmetries of field theoretic models. It can be used for projection²⁵ of these states onto eigenstates of the appropriate symmetries, and it can also provide a starting point for descriptions of the scattering of solitons.⁶⁶ The generator-coordinate method,²⁴ which has been widely used in nuclear physics,²⁰ is thus an attractive alternative to collective coordinate approaches in field theories. In some cases, the collective methods become very complicated; in others they rely on semiclassical assumptions which may not be justified.

Here I have applied this method to a chiral model^{8,9} of the nucleon and Δ . A coherent state is used to describe a hedgehog baryon, and this is projected onto spin-isospin eigenstates. The N and Δ wave functions are varied after projection. The resulting N - Δ splitting is about half the observed value, suggesting the need for residual, spin-dependent gluonic interactions. The calculated nucleon

properties are in reasonable agreement with experiment, and are similar to those obtained in earlier MFA calculations.⁸ The quantum treatment of the pions means that their contributions to charge radii can be calculated in the present approach. The model nucleon wave function contains about one pion on average; this is comparable to the cloudy bag model.³² Because of the small numbers of quanta in realistic nucleon wave functions, semiclassical methods, such as used in the Skyrme model,¹³⁻¹⁶ are expected to yield poor results.

The coherent state can also be projected onto eigenstates of linear momentum. This needs to be done, since there may be significant center-of-mass corrections to nucleon properties. (Such calculations have already been made in the soliton bag model.²¹) One should also explore more general trial functions,⁴³ which do not rely on the hedgehog ansatz. The present calculations need to be extended to include vector mesons, since these have been shown to have important effects on some nucleon properties in this model.¹⁰

Finally, the effects of vacuum polarization needed to be studied. The work of Ripka and Kahana^{47,50} has shown that inclusion of the Dirac sea can significantly change the detailed forms of the quark density distributions and contributions to the total energy in this type of soliton. Also, the noninteracting basis used here to expand the meson fields needs to be improved on: a one-loop calculation should be done to investigate the effects of distortion of the meson vacuum.

ACKNOWLEDGMENTS

I am grateful to L. Wilets for numerous discussions and debates about hedgehogs, coherent states, and related ideas. I also acknowledge useful discussions with M. Banerjee, W. Broniowski, T. Cohen, M. Harvey, A. D. Jackson, G. Miller, and J. Parmentola, as well as advice on computing matters from G. Lübeck. I am indebted to M. Rosina for pointing out an error in an earlier version of this paper, and for a copy of Ref. 67, which is very similar to the present work. I am grateful for the hospitality of the Lewes Center for Physics, where this work was initiated. This work was supported in part by the U. S. Department of Energy.

APPENDIX

In this appendix I give details of the calculation of expectation values of various operators in the projected states, using the formulas (4.10) and (4.13).

The normalization integral in those expressions is

$$\mathcal{N}_J = \int d^3\Omega D_{J,J}^J(\Omega) \langle H | \hat{R}(\Omega)^{-1} | H \rangle. \quad (\text{A1})$$

The overlap between the rotated and unrotated hedgehog states can be calculated using (2.7), the definition (3.2), and the overlap between rotated hedgehog spinors:

$$\chi_h^\dagger \hat{R}(\Omega)^{-1} \chi_h = \cos \frac{\beta}{2} \cos \frac{\alpha+\gamma}{2}. \quad (\text{A2})$$

This gives

$$\begin{aligned} & \langle H | \hat{R}(\Omega)^{-1} | H \rangle \\ &= \left[\cos \frac{\beta}{2} \cos \frac{\alpha + \gamma}{2} \right]^3 \\ & \times \exp \left[\bar{N}_\sigma + \frac{\bar{N}_\pi}{3} \left[4 \cos^2 \frac{\beta}{2} \cos^2 \frac{\alpha + \gamma}{2} - 1 \right] \right], \quad (\text{A3}) \end{aligned}$$

where α , β , and γ are the usual Euler angles.⁵¹ The D function has the form⁵¹

$$D_{J,J}^J(\Omega) = e^{-iJ(\alpha+\gamma)(\cos\beta/2)^{2J}}, \quad (\text{A4})$$

and so the integrand in (A1) does not depend on $\alpha - \gamma$. Hence the integration over $\alpha - \gamma$ is trivial. The integral over β can be done analytically, and leads to

$$\mathcal{N}_J = 4\pi \exp(\bar{N}_\sigma - \frac{1}{3}\bar{N}_\pi) \int_0^{2\pi} d\bar{\alpha} \cos(2J\bar{\alpha}) \cos^3 \bar{\alpha} I \left[\frac{2J+3}{2}; \frac{4}{3}\bar{N}_\pi \cos^2 \bar{\alpha} \right], \quad (\text{A5})$$

where

$$I(n; a) \equiv \frac{1}{2} \int_0^\pi d\beta \sin\beta \left[\cos \frac{\beta}{2} \right]^{2n} \exp \left[a \cos^2 \frac{\beta}{2} \right] = \frac{d^n}{da^n} \left[\frac{e^a - 1}{a} \right]. \quad (\text{A6})$$

The integral over $\bar{\alpha}$ must be done numerically. In the present calculations 20 points were used, equally spaced between zero and $\pi/2$ (due to the symmetry of the integral).

Using the form of the quark single-particle wave functions (3.3), the quark pieces of the mean-square charge radii can be written

$$\begin{aligned} & \langle JMM_T | \int d^3r r^2 \mathcal{Q}_{EM}^0 | JMM_T \rangle \\ &= \int r^4 dr (u^2 + v^2) \left(\frac{1}{2} + \langle JMM_T | \mathcal{Q}_{T_3} | JMM_T \rangle \right), \quad (\text{A7}) \end{aligned}$$

where \mathcal{Q}_{T_3} is the third component of the total quark isospin operator:

$$\mathcal{Q}_{T_3} = \frac{1}{2} \int d^3r \psi^\dagger \tau_3 \psi. \quad (\text{A8})$$

The quark pieces of the expectation values of various vector operators are

$$\begin{aligned} & \langle JMM_T | \int d^3r \frac{1}{2} (\mathbf{r} \times \mathcal{Q}_{EM})_z | JMM_T \rangle \\ &= \frac{2}{3} \int r^3 dr uv \langle JMM_T | \frac{1}{3} \mathcal{Q}_{S_z} + \mathcal{Q}_{G_3^z} | JMM_T \rangle, \quad (\text{A9}) \end{aligned}$$

$$\begin{aligned} & \langle JMM_T | \int d^3r \mathcal{Q}_{A_3^z} | JMM_T \rangle \\ &= \int r^2 dr (u^2 - \frac{1}{3}v^2) \langle JMM_T | \mathcal{Q}_{G_3^z} | JMM_T \rangle, \quad (\text{A10}) \end{aligned}$$

$$\begin{aligned} & \langle JMM_T | \int d^3r z \mathcal{Q}_{j_{\pi 3}} | JMM_T \rangle \\ &= -g \frac{4}{3} \int r^3 dr uv \langle JMM_T | \mathcal{Q}_{G_3^z} | JMM_T \rangle, \quad (\text{A11}) \end{aligned}$$

where the total quark spin is

$$\mathcal{Q}_S = \frac{1}{2} \int d^3r \psi^\dagger \boldsymbol{\sigma} \psi, \quad (\text{A12})$$

and the ‘‘Gamow-Teller’’ operator is

$$\mathcal{Q}_{G_3} = \frac{1}{2} \int d^3r \psi^\dagger \boldsymbol{\sigma} \tau_3 \psi. \quad (\text{A13})$$

From the definition of the hedgehog spinor (3.4), one finds that

$$\chi_h^\dagger \hat{R}(\Omega)^{-1} \tau_3 \chi_h = -i \sin \frac{\alpha + \gamma}{2} \cos \frac{\beta}{2}, \quad (\text{A14})$$

and so the total quark isospin is found to be

$$\begin{aligned} & \langle JM - M | \mathcal{Q}_{T_3} | JM - M \rangle \\ &= -i \frac{3}{2\mathcal{N}_J} \int d^3\Omega D_{M,M}^J(\Omega) \tan \frac{\alpha + \gamma}{2} \\ & \times \langle H | \hat{R}(\Omega)^{-1} | H \rangle. \quad (\text{A15}) \end{aligned}$$

The integral over Euler angles can be done in a similar manner to the normalization integral.

The total quark spin can be calculated using

$$\chi_h^\dagger \hat{R}(\Omega)^{-1} \sigma_{1m} \chi_h = \frac{\sqrt{3}}{2} \sum_{\mu, \mu'} \langle \frac{1}{2} \mu 1 m | \frac{1}{2} \mu' \rangle D_{\mu', \mu}^{1/2}(\Omega)^*, \quad (\text{A16})$$

in (4.13). After recoupling the D functions, one obtains

$$\begin{aligned} & \langle JM - M | \mathcal{Q}_{S_3} | JM - M \rangle = \frac{3}{2\mathcal{N}_J} \left[\frac{3(2J+1)}{2} \right]^{1/2} \sum_{\mu, J', M'} \langle JM \frac{1}{2} - \mu | J' M' \rangle^2 (-1)^{J+J'-1/2} \begin{Bmatrix} \frac{1}{2} & \frac{1}{2} & 1 \\ J & J & J' \end{Bmatrix} \\ & \times \int d^3\Omega D_{M', M}^{J'}(\Omega) \frac{\langle H | \hat{R}(\Omega)^{-1} | H \rangle}{\cos \frac{\beta}{2} \cos \frac{\alpha + \gamma}{2}}. \quad (\text{A17}) \end{aligned}$$

The expectation value of the Gamow-Teller operator can be evaluated similarly, using

$$\chi_h^\dagger \hat{R}(\Omega)^{-1} \sigma_{1m} \tau_3 \chi_h = \frac{\sqrt{3}}{2} \sum_{\mu, \mu'} (-1)^{1/2-\mu} \langle \frac{1}{2} \mu 1 m | \frac{1}{2} \mu' \rangle D_{\mu', \mu}^{1/2}(\Omega)^* . \quad (\text{A18})$$

This leads to an expression for $\langle JM - M | \mathcal{O}G_3^z | JM - M \rangle$ which is almost identical to (A16), differing only by a factor of $(-1)^{1/2-\mu}$ in the sum over μ .

In calculating the energy of a projected state, it is convenient to group the pionic terms into the free pion Hamiltonian, a second-order, and a fourth-order interaction. Terms which do not involve the pion field (such as the quark and σ kinetic energies) are not affected by projection. The pionic terms can be evaluated using the analogues of (2.8) and (2.9) for rotated and unrotated hedgehog states:

$$\langle H | \hat{R}(\Omega)^{-1} \phi(\mathbf{r}) | H \rangle = \frac{1}{2} [\hat{\mathbf{r}} + \mathbf{O}(\Omega)^{-1} \hat{\mathbf{r}}] h(r) \langle H | \hat{R}(\Omega)^{-1} | H \rangle , \quad (\text{A19})$$

$$\langle H | \hat{R}(\Omega)^{-1} \boldsymbol{\pi}(\mathbf{r}) | H \rangle = -i \frac{1}{2} [\hat{\mathbf{r}} + \mathbf{O}(\Omega)^{-1} \hat{\mathbf{r}}] h_\omega(r) \langle H | \hat{R}(\Omega)^{-1} | H \rangle , \quad (\text{A20})$$

along with similar expressions for higher powers of the field operators. Here $h_\omega(r)$ is defined by (5.5), and $\mathbf{O}(\Omega)$ is the SO(3) matrix representation of $\hat{R}(\Omega)$.

The quark-pion coupling term involves

$$\langle H | \hat{R}(\Omega)^{-1} i \bar{\psi}(\mathbf{r}) \boldsymbol{\tau} \cdot \boldsymbol{\phi}(\mathbf{r}) \gamma_5 \psi(\mathbf{r}) | H \rangle = -\frac{6}{4\pi} u(r) v(r) h(r) \chi_h^\dagger \hat{R}(\Omega)^{-1} (\hat{\mathbf{r}} \cdot \boldsymbol{\sigma}) \frac{1}{2} [\hat{\mathbf{r}} + \mathbf{O}(\Omega)^{-1} \hat{\mathbf{r}}] \cdot \boldsymbol{\tau} \chi_h \frac{\langle H | \hat{R}(\Omega)^{-1} | H \rangle}{\cos \frac{\beta}{2} \cos \frac{\alpha + \gamma}{2}} . \quad (\text{A21})$$

Using (3.5) and the analogous relation for $\hat{R}(\Omega) \chi_h$,

$$[\mathbf{O}(\Omega)^{-1} \boldsymbol{\sigma} + \boldsymbol{\tau}] \hat{R}(\Omega) \chi_h = 0 , \quad (\text{A22})$$

(A21) can be written as

$$\langle H | \hat{R}(\Omega)^{-1} i \bar{\psi}(\mathbf{r}) \boldsymbol{\tau} \cdot \boldsymbol{\phi}(\mathbf{r}) \gamma_5 \psi(\mathbf{r}) | H \rangle = \frac{6}{4\pi} u(r) v(r) h(r) \langle H | \hat{R}(\Omega)^{-1} | H \rangle . \quad (\text{A23})$$

This shows that the quark-pion term also is unaffected by projection, as noted in Ref. 67.

Since the σ part of the wave function is unaffected by projection, the σ field can be treated as a c -number function. Using (A19), the second-order interaction term can be written

$$\begin{aligned} \left\langle JJ - J \left| \int d^3 r : \sigma(\mathbf{r})^2 \phi(\mathbf{r})^2 : \right| JJ - J \right\rangle &= \frac{1}{\mathcal{N}_J} \int d^3 r \sigma_0(r)^2 h(r)^2 \int d^3 \Omega D_{J,J}^J(\Omega) \frac{1}{2} [1 + \hat{\mathbf{r}} \cdot \mathbf{O}(\Omega) \hat{\mathbf{r}}] \langle H | \hat{R}(\Omega)^{-1} | H \rangle \\ &= C_2(J; \bar{N}_\pi) 4\pi \int r^3 dr \sigma_0(r)^2 h(r)^2 , \end{aligned} \quad (\text{A24})$$

where the projection coefficient is defined by

$$C_2(J; \bar{N}_\pi) \equiv \frac{1}{3\mathcal{N}_J} \int d^3 \Omega D_{J,J}^J(\Omega) \left[1 + 2 \left[\cos \frac{\beta}{2} \cos \frac{\alpha + \gamma}{2} \right]^2 \right] \langle H | \hat{R}(\Omega)^{-1} | H \rangle . \quad (\text{A25})$$

The fourth-order interaction term can be evaluated similarly to get

$$\left\langle JJ - J \left| \int d^3 r : \phi(\mathbf{r})^4 : \right| JJ - J \right\rangle = C_4(J; \bar{N}_\pi) 4\pi \int r^2 dr h(r)^4 , \quad (\text{A26})$$

where

$$C_4(J; \bar{N}_\pi) \equiv \frac{1}{15\mathcal{N}_J} \int d^3 \Omega D_{J,J}^J(\Omega) \left[3 + 4 \left[\cos \frac{\beta}{2} \cos \frac{\alpha + \gamma}{2} \right]^2 + 8 \left[\cos \frac{\beta}{2} \cos \frac{\alpha + \gamma}{2} \right]^4 \right] \langle H | \hat{R}(\Omega)^{-1} | H \rangle . \quad (\text{A27})$$

The noninteracting term is most easily evaluated by using the fact that it is diagonal in the basis used to expand the pion field:

$$:H_0: = \int d^3 k \omega_{\pi k} \mathbf{a}^\dagger(\mathbf{k}) \cdot \mathbf{a}(\mathbf{k}) . \quad (\text{A28})$$

This term in the energy can be written

$$\left\langle JJ - J \left| \int d^3 r : H_0 : \right| JJ - J \right\rangle = C_0(J; \bar{N}_\pi) 4\pi \int r^2 dr \left[\left[\frac{\partial h}{\partial r} \right]^2 + \frac{2}{r^2} h^2 + m_\pi^2 h^2 \right] , \quad (\text{A29})$$

where

$$C_0(J; \bar{N}_\pi) \equiv \frac{1}{3\mathcal{N}_J} \int d^3\Omega D_{J,J}^J(\Omega) \left[4 \left[\cos \frac{\beta}{2} \cos \frac{\alpha+\gamma}{2} \right]^2 - 1 \right] \langle H | \hat{R}(\Omega)^{-1} | H \rangle. \quad (\text{A30})$$

The pion number operator has the same form as (A28) (without the factor of $\omega_{\pi k}$). Hence the average number of pions in the projected state, Eq. (4.15), is also multiplied by $C_0(J; \bar{N}_\pi)$.

The pionic contribution to the charge density operator [the time-component of (6.1)] is

$${}^M J_{\text{EM}}^0 =: [\boldsymbol{\phi} \times \boldsymbol{\pi}]_3: . \quad (\text{A31})$$

Hence, from (2.19) and (2.20), the meson contribution to the mean-square charge radius is

$$\begin{aligned} \langle JM-M | \int d^3r r^2 {}^M J_{\text{EM}}^0 | JM-M \rangle &= i \frac{1}{2\mathcal{N}_J} \int d^3r r^2 h(r) h_\omega(r) \int d^3\Omega D_{M,M}^J(\Omega) \hat{\mathbf{r}} \times \mathbf{O}(\Omega)^{-1} \hat{\mathbf{r}} \langle H | \hat{R}(\Omega)^{-1} | H \rangle \\ &= C_{\text{ch}}(J, -M; \bar{N}_\pi) \frac{8\pi}{3} \int r^4 dr h(r) h_\omega(r), \end{aligned} \quad (\text{A32})$$

where

$$C_{\text{ch}}(J, -M; \bar{N}_\pi) \equiv -i \frac{1}{\mathcal{N}_J} \int d^3\Omega D_{M,M}^J(\Omega) \sin \frac{\alpha+\gamma}{2} \cos \frac{\alpha+\gamma}{2} \left[\cos \frac{\beta}{2} \right]^2 \langle H | \hat{R}(\Omega)^{-1} | H \rangle. \quad (\text{A33})$$

The simplest vector operators to consider are ones which are linear in the pion field. These are of the form

$$\mathbf{V} = \int d^3r \hat{\mathbf{r}} f(r) \phi_3(\mathbf{r}), \quad (\text{A34})$$

where $f(r)$ is either a spherically symmetric c -number function, or depends only on the σ field. In evaluating matrix elements of vector operators, it is convenient to rewrite (A19) in spherical notation:

$$\langle H | \hat{R}(\Omega)^{-1} \phi_{1m}(\mathbf{r}) | H \rangle = \frac{1}{2} \left[r_{1m} + \sum_{m'} r_{1m'} D_{m',m}^1(\Omega) \right] \frac{h(r)}{r} \langle H | \hat{R}(\Omega)^{-1} | H \rangle. \quad (\text{A35})$$

Hence the matrix element of \mathbf{V} between rotated and unrotated hedgehogs is

$$\langle H | \hat{R}(\Omega)^{-1} V_{1m} | H \rangle = \frac{2\pi}{3} \int r^2 dr f(r) h(r) [\delta_{m,0} + (-1)^m D_{-m,0}^1(\Omega)] \langle H | \hat{R}(\Omega)^{-1} | H \rangle. \quad (\text{A36})$$

Using this in (4.13) and recoupling the D functions, one finds that both terms of (A36) give the same contribution. Hence the expectation value of V_3 in an eigenstate is

$$\langle JM-M | V_3 | JM-M \rangle = \langle JM10 | JM \rangle^2 \frac{4\pi}{3} \int r^2 dr f(r) h(r). \quad (\text{A37})$$

This is the form used for the calculation of mesonic pieces of vector operators in Ref. 8 [see Eq. (3.13) of that paper].

The axial-vector coupling constant can be calculated using $f(r) = 2\partial\sigma_0/\partial r$ in (A37). The pion coupling (6.8) is obtained for $f(r) = r$, and the first-order piece of (6.9) for $f(r) = -\lambda^2(\sigma_0^2 - F_\pi^2)$.

The calculation of $g_{\pi NN}$ from (6.9) also involves a term which is third-order in the pion field. This can be evaluated from (4.13) and

$$\begin{aligned} \left\langle H \left| \hat{R}(\Omega)^{-1} \int d^3r r_{1m} \phi(\mathbf{r})^3 \right| H \right\rangle &= \frac{1}{4} \int d^3r \left[\frac{h(r)}{r} \right]^3 r_{1m} \left[r^2 + \sum_{\mu,\mu'} r_{1\mu} D_{\mu,\mu'}^1(\Omega) (-1)^{\mu'} r_{1-\mu'} \right] \\ &\quad \times \left[r_{10} + \sum_{\nu} r_{1\nu} D_{\nu,0}^1(\Omega) \right] \langle H | \hat{R}(\Omega)^{-1} | H \rangle \\ &= \frac{\pi}{15} \int r^3 dr h(r)^3 \left[6\delta_{m,0} + 6(-1)^m D_{-m,0}^1(\Omega) \right. \\ &\quad \left. + \delta_{m,0} \sum_{\mu} D_{\mu,\mu}^1(\Omega) + (-1)^m D_{-m,0}^1(\Omega) \sum_{\mu} D_{\mu,\mu}^1(\Omega) \right. \\ &\quad \left. + D_{0,m}^1(\Omega) + (-1)^m \sum_{\mu} D_{-m,\mu}^1(\Omega) D_{\mu,0}^1(\Omega) \right]. \end{aligned} \quad (\text{A38})$$

After recoupling, and using the fact that $\int d^3\Omega D_{M,M}^J(\Omega)\langle H|\hat{R}(\Omega)^{-1}|H\rangle$ is independent of M , one obtains

$$\begin{aligned} & \left\langle JM-M \left| \int d^3r z \phi(\mathbf{r})^3 \right| JM-M \right\rangle \\ &= \langle JM10 | JM \rangle^2 \frac{\pi}{15} \int r^3 dr h(r)^3 \left[12 + \frac{2}{\mathcal{N}_J} \sum_{J'} \left\{ \frac{2J'+1}{2J+1} + (-1)^{2J}(2J'+1) \begin{Bmatrix} J & J & 1 \\ J & J' & 1 \end{Bmatrix} \right\} \right] \\ & \quad \times \int d^3\Omega D_{J',J'}^{J'}(\Omega) \langle H | \hat{R}(\Omega)^{-1} | H \rangle \Bigg]. \quad (\text{A39}) \end{aligned}$$

Finally, the meson pieces of the magnetic moments are obtained from

$$\begin{aligned} & - \left\langle H \left| \hat{R}(\Omega)^{-1} \int d^3r \epsilon_{3\alpha\beta} \phi_\alpha(\mathbf{r})(\mathbf{r} \times \nabla)_{1m} \phi_\beta(\mathbf{r}) \right| H \right\rangle \\ &= \frac{2\pi}{3} \int r^2 dr h(r)^2 (-1)^m \sum_{\mu,\mu',\nu,\nu'} \langle 1\mu 1\mu' | 1m \rangle \langle 1\nu 1\nu' | 10 \rangle [\delta_{\mu,-\nu} \delta_{\mu',-\nu'} + \delta_{\mu,-\nu} D_{-\mu',\nu}^1(\Omega) \\ & \quad + \delta_{\mu',-\nu} D_{-\mu,\nu}^1(\Omega) + D_{-\mu,\nu}^1(\Omega) D_{-\mu',\nu}^1(\Omega)]. \quad (\text{A40}) \end{aligned}$$

Inserting this into (4.13), and recoupling, gives

$$\begin{aligned} & \frac{1}{2} \left\langle JM-M \left| \int d^3r (\mathbf{r} \times \mathbf{J}_{EM})_z \right| JM-M \right\rangle \\ &= - \langle JM10 | JM \rangle^2 \frac{2\pi}{3} \int r^2 dr h(r)^2 \\ & \quad \times \left[1 + \frac{3}{\mathcal{N}_J} \sum_{J'} (2J'+1) \begin{Bmatrix} 1 & 1 & 1 \\ J & J & J' \end{Bmatrix}^2 \int d^3\Omega D_{J',J'}^{J'}(\Omega) \langle H | \hat{R}(\Omega)^{-1} | H \rangle \right]. \quad (\text{A41}) \end{aligned}$$

*Present address: Department of Theoretical Physics, Schuster Laboratory, University of Manchester, Manchester, M13 9PL, U.K.

¹For a review, see W. Marciano and H. Pagels, Phys. Rep. **36C**, 137 (1978).

²M. Creutz, *Quarks, Gluons, and Lattices* (Cambridge University Press, New York, 1983).

³*Solitons in Nuclear and Elementary Particle Physics*, proceedings of the 1984 Lewes Workshop, edited by A. Chodos, E. Hadjimichael, and H. C. Tze (World Scientific, Singapore, 1984).

⁴T. D. Lee and G. C. Wick, Phys. Rev. D **9**, 2291 (1974).

⁵W. A. Bardeen, M. S. Chanowitz, S. D. Drell, M. Weinstein, and T. M. Yan, Phys. Rev. D **11**, 1094 (1975).

⁶R. Friedberg and T. D. Lee, Phys. Rev. D **15**, 1694 (1977); **16**, 1096 (1977); **18**, 2623 (1978).

⁷R. Goldflam and L. Wilets, Phys. Rev. D **25**, 1951 (1982).

⁸M. C. Birse and M. K. Banerjee, Phys. Lett. **136B**, 284 (1984); Phys. Rev. D **31**, 118 (1985).

⁹S. Kahana, G. Ripka, and V. Soni, Nucl. Phys. **A415**, 351 (1984).

¹⁰W. Broniowski and M. K. Banerjee, Phys. Lett. **158B**, 335 (1985).

¹¹R. Seki and S. Ohta, Nucl. Phys. **A437**, 541 (1985); and a contribution to Ref. 3.

¹²L. S. Celenza and C. M. Shakin, Phys. Rev. C **28**, 2042 (1983); and a contribution to Ref. 3.

¹³T. H. R. Skyrme, Proc. R. Soc. London **A260**, 127 (1961); Nucl. Phys. **31**, 556 (1962).

¹⁴G. S. Adkins, C. R. Nappi, and E. Witten, Nucl. Phys. **B228**, 552 (1983); G. S. Adkins and C. R. Nappi, *ibid.* **B233**, 109 (1984); see also various contributions to Ref. 3.

¹⁵A. D. Jackson and M. Rho, Phys. Rev. Lett. **51**, 751 (1983).

¹⁶G. S. Adkins and C. R. Nappi, Phys. Lett. **137B**, 251 (1984).

¹⁷S. Coleman, in *New Phenomena in Subnuclear Physics*, edited by A. Zichichi (Plenum, New York, 1977).

¹⁸T. D. Lee, *Particle Physics and Introduction to Field Theory* (Harwood Academic, New York, 1981).

¹⁹A. Chodos and C. B. Thorn, Phys. Rev. D **12**, 2733 (1975).

²⁰P. Ring and P. Schuck, *The Nuclear Many-Body Problem* (Springer, Berlin, 1980).

²¹(a) M. C. Birse, E. M. Henley, G. Lübeck, and L. Wilets, contribution to Ref. 3; E. G. Lübeck *et al.*, Phys. Rev. D **33**, 234 (1986); (b) L. Wilets, Int. J. Theor. Phys. (to be published).

²²See Ref. 20, Sec. 11.3, for a discussion of collective coordinate methods in nuclear physics.

²³For a review, see R. Rajaraman, *Solitons and Instantons* (North-Holland, Amsterdam, 1982).

²⁴D. L. Hill and J. A. Wheeler, Phys. Rev. **89**, 1102 (1953).

²⁵R. E. Peierls and J. Yoccoz, Proc. Phys. Soc. London **A70**, 381 (1957); J. J. Griffin and J. A. Wheeler, Phys. Rev. **108**, 211 (1957).

²⁶T. D. Lee, F. E. Low, and D. Pines, Phys. Rev. **90**, 297 (1953); T. D. Lee and D. Pines, *ibid.* **92**, 883 (1953).

- ²⁷J. R. Klauder, *Ann. Phys. (N.Y.)* **11**, 123 (1960); R. J. Glauber, *Phys. Rev.* **131**, 2766 (1963).
- ²⁸Reference 17 contains an early discussion of the coherent-state description of solitons.
- ²⁹J. da Providencia, *Nucl. Phys.* **B57**, 536 (1973).
- ³⁰K. Huang and D. R. Stump, *Phys. Rev. D* **14**, 223 (1976).
- ³¹J. N. Urbano and K. Goeke, *Phys. Lett.* **143B**, 319 (1984); *Phys. Rev. D* **32**, 2396 (1985); B. Golli, M. Rosina, and J. da Providencia, *Nucl. Phys.* **A436**, 733 (1985); see also J. da Providencia and J. Urbano, *Phys. Rev. D* **18**, 4208 (1978).
- ³²G. A. Miller, A. W. Thomas, and S. Th  berge, *Phys. Lett.* **91B**, 192 (1980); for reviews, see A. W. Thomas, *Adv. Nucl. Phys.* **13**, 1 (1983); G. A. Miller, *International Review of Nuclear Physics*, edited by W. Weise (World Scientific, Singapore, 1984), Vol. 1.
- ³³S. Coleman, J. Wess, and B. Zumino, *Phys. Rev.* **177**, 2239 (1969).
- ³⁴D. I. Kazakov, V. N. Pervushin, and S. V. Pushkin, *J. Phys. A* **11**, 2093 (1978).
- ³⁵M. Gell-Mann and M. L  vy, *Nuovo Cimento* **16**, 705 (1960).
- ³⁶J. Finger, D. Horn, and J. E. Mandula, *Phys. Rev. D* **20**, 3253 (1979); J. Finger, J. E. Mandula, and J. Weyers, *Phys. Lett.* **96B**, 367 (1980).
- ³⁷T. Goldman and R. W. Haymaker, *Phys. Rev. D* **22**, 724 (1981).
- ³⁸V. A. Miransky, V. P. Gusynin, and Y. A. Sitenko, *Phys. Lett.* **100B**, 157 (1981); V. A. Miransky and P. I. Fomin, *ibid.* **105B**, 387 (1981); V. P. Gusynin, V. A. Miransky, and Y. A. Sitenko, *ibid.* **123B**, 428 (1983).
- ³⁹Y. Nambu and G. Jona-Lasinio, *Phys. Rev.* **122**, 345 (1961); **124**, 246 (1961).
- ⁴⁰See, for example, P. Ramond, *Field Theory: A Modern Primer* (Benjamin/Cummings, Reading, Mass., 1981).
- ⁴¹J. M. Cornwall, R. Jackiw, and E. Tomboulis, *Phys. Rev. D* **10**, 2428 (1974); S. Coleman, R. Jackiw, and H. Politzer, *ibid.* **10**, 2491 (1974); S.-J. Chang, *ibid.* **12**, 1071 (1975); T. Barnes and G. I. Ghandour, *ibid.* **22**, 924 (1980).
- ⁴²M. Bolsterli, *Phys. Rev. D* **24**, 400 (1981).
- ⁴³U.-J. Weise, Th. K  ppel, and M. Harvey, Chalk River report, 1984 (unpublished).
- ⁴⁴M. Fiolhais, J. N. Urbano, and K. Goeke, *Phys. Lett.* **150B**, 253 (1985).
- ⁴⁵W. Pauli and S. N. Dancoff, *Phys. Rev.* **62**, 85 (1942).
- ⁴⁶J. A. Parmentola, *Phys. Rev. D* **27**, 2686 (1983); **29**, 2563 (1984).
- ⁴⁷S. Kahana and G. Ripka, *Nucl. Phys.* **A429**, 462 (1984).
- ⁴⁸The situation is analogous to that of electron orbitals in the presence of a charge $150 < Z < 170$. There, too, it is convenient to use an uncharged vacuum as a reference state, although the state with all negative-energy orbitals occupied has nonzero charge. See J. Reinhardt, B. M  ller, and W. Greiner, *Phys. Rev. A* **24**, 103 (1981); M. Soffel, B. M  ller, and W. Greiner, *Phys. Rep.* **85**, 51 (1982), and references therein.
- ⁴⁹J. Goldstone and F. Wilczek, *Phys. Rev. Lett.* **47**, 986 (1981).
- ⁵⁰G. Ripka and S. Kahana, *Phys. Lett.* **155B**, 327 (1985).
- ⁵¹The definitions and conventions used for rotation operators, etc., are (apart from some minor differences of notation) those in D. M. Brink and G. R. Satchler, *Angular Momentum*, 2nd ed. (Oxford University Press, Oxford, England, 1968).
- ⁵²U. Ascher, J. Christiansen, and R. D. Russel, *A. C. M. Trans. Math. Software* **7**, 209 (1981).
- ⁵³Th. K  ppel and M. Harvey, *Phys. Rev. D* **31**, 171 (1985).
- ⁵⁴M. K. Banerjee and J. B. Cammarata, *Phys. Rev. D* **18**, 4078 (1978).
- ⁵⁵V. P. Efrosinin and D. A. Zaikin, *Yad. Fiz.* **35**, 1546 (1982) [*Sov. J. Nucl. Phys.* **35**, 904 (1982)]; *Yad. Fiz.* **39**, 115 (1984) [*Sov. J. Nucl. Phys.* **39**, 71 (1984)].
- ⁵⁶J. F. Donoghue and K. Johnson, *Phys. Rev. D* **21**, 1975 (1980); C. W. Wong, *ibid.* **24**, 1416 (1981).
- ⁵⁷A. W. Thomas, *Phys. Lett.* **126B**, 97 (1983).
- ⁵⁸V. Vento, M. Rho, E. B. Nyman, J. H. Jun, and G. E. Brown, *Nucl. Phys.* **A345**, 413 (1980).
- ⁵⁹D. Finkelstein and J. Rubinstein, *J. Math. Phys.* **9**, 1762 (1968).
- ⁶⁰E. Witten, *Nucl. Phys.* **B223**, 422 (1983); **B223**, 433 (1983).
- ⁶¹I. J. R. Aitchison and C. M. Fraser, *Phys. Lett.* **146B**, 63 (1984).
- ⁶²J. D. Breit and C. R. Nappi, *Phys. Rev. Lett.* **53**, 889 (1984); C. Hajduk and B. Schwesinger, *Phys. Lett.* **140B**, 172 (1984); A. Hayashi, G. Eckart, G. Holzwarth, and H. Walliser, *ibid.* **147B**, 5 (1984); H. Walliser and G. Eckart, *Nucl. Phys.* **A429**, 514 (1984); I. Zahed, U.-G. Meissner, and U. B. Kaulfuss, *ibid.* **B426**, 525 (1984); J. Dey and J. Le Tourneux, Montreal report, 1984 (unpublished); K. F. Liu, J. S. Zhang, and G. R. E. Black, *Phys. Rev. D* **30**, 2015 (1984); L. C. Biedenharn, Y. Dothan, and M. Tarlini, *ibid.* **31**, 649 (1985); M. Mattis and M. Karliner, *ibid.* **31**, 2833 (1985).
- ⁶³G. 't Hooft, *Nucl. Phys.* **B72**, 461 (1974); **B75**, 461 (1975); E. Witten, *ibid.* **B160**, 57 (1979).
- ⁶⁴J. A. Parmentola, *Phys. Rev. D* **30**, 685 (1984); K. Bardakci, *Nucl. Phys.* **B243**, 197 (1984); see also J. L. Gervais and B. Sakita, *Phys. Rev. Lett.* **52**, 87 (1984).
- ⁶⁵E. Braaten and J. P. Ralston, *Phys. Rev. D* **31**, 598 (1985); and a contribution to Ref. 3.
- ⁶⁶L. Wilets, in *Hadrons and Heavy Ions*, advanced course in theoretical physics, Cape Town, 1984, edited by W. D. Heiss (Lecture Notes in Physics, No. 231) (Springer, Berlin, 1985).
- ⁶⁷B. Golli and M. Rosina, Ljubljana report, 1985 (unpublished).